

V. D. Jović · V. Maksimović · M. G. Pavlović
K. I. Popov

Morphology, internal structure and growth mechanism of electrodeposited Ni and Co powders

Received: 3 January 2005 / Revised: 8 March 2005 / Accepted: 23 March 2005 / Published online: 20 July 2005
© Springer-Verlag 2005

Abstract In this paper the morphology (SEM analysis), the internal structure (cross-section analysis) and the growth mechanism of Ni and Co powders electrodeposited from ammoniacal electrolyte are investigated. It is shown that morphology and the internal structure of those powders are quite different. For Ni powder, all particles are of the same morphology, cauliflower-like type. In the case of Co powder, generally two types of particles are detected: (1) dendrite particles and (2) different types of agglomerates, compact, spongy-like and ball-like ones. The growth mechanism for all agglomerates is based on the fact that with the time of growth the disperse (dendrite) agglomerate is branching in different directions and at the tip of each branch spherical diffusion takes over the planar one, providing conditions for the growth of compact deposit. After some time, these branches form compact deposit all over the agglomerate surface and the same agglomerate further grows as a compact one, until it falls off from the electrode surface. Characteristic of all agglomerates is the presence of deep cavities on their surface and the fern-like dendrites on the bottom for most of these cavities.

Keywords Ni · Co · Powders · Dendrite particles · Cauliflower-like particles · Different agglomerates · Growth mechanism

Introduction

Almost all data concerning Ni powder electrodeposition are summarized in the chapter XVIII of the book “Electrodeposition of Powders from Solutions”, by Calusaru [1]. Two types of electrolyte for Ni powder electrodeposition were investigated: Acid electrolytes [2–10] and ammoniacal electrolytes [2, 5, 11]. For acid electrolytes it is characteristic that the increase of current density and decrease of nickel ion concentration in solution cause a lowering of powder fragility. The powder is free from oxides and basic salts and dry powder could be stored in a dry place indefinitely without oxidation or structure change [2–10]. Characteristic of ammoniacal electrolytes is that the increase of ammonia concentration cause disperse and pure (without hydroxide impurities) deposit formation consisting of dark nickel particles of 4–10 μm and of larger particles of about 400 μm [2, 5, 11].

The influence of pulsating and reversing current regime on the Ni powder electrodeposition was investigated in the paper of Pavlović et al. [12]. It is found that the increase of frequency of pulsating current induces a decrease in particle size, while in the case of reversing current regimes the size of powder particles increase with increasing average current density.

According to Calusaru [1] some information on electrodeposition of Co powder are available in patents [13] as well as in reviews [14]. Unfortunately these references are from 1932 and there are no data about morphology of powder particles, while since then there are no published data about electrodeposition of Co powder. Only two micrographs of Co powder, showing that the particles are very fine agglomerates, are presented in the Metallographic Atlas of Powder

V. D. Jović
Center for Multidisciplinary Studies, University of Belgrade,
11030 Belgrade, P. O. Box 33, Serbia & Montenegro

V. Maksimović
Institute of Nuclear Science, “Vinča”,
11001 Belgrade, P. O. Box 522,
Serbia & Montenegro

M. G. Pavlović (✉)
ICTM, Institute of Electrochemistry,
11000 Belgrade, Njegoševa 12,
Serbia & Montenegro
E-mail: duki@elab.tmf.bg.ac.yu
Tel.: +381-11-3370430
Fax: +381-11-3370389

K. I. Popov
Faculty of Technology and Metallurgy,
University of Belgrade, 11000 Belgrade,
Karnegijeva 4, Serbia & Montenegro

Metallurgy [15], but the procedure of their production is not mentioned and it is stated that their typical application is for hard metal production.

In this paper results on the investigation of the morphology, internal structure and growth mechanism of electrodeposited Ni and Co powders are presented.

Experimental

All powder samples were electrodeposited at the temperature of about 50 °C in the cylindrical glass cell of the total volume of 1 l with cone shaped bottom of the cell in order to collect powder particles in it. Working electrode was a glassy carbon rod of the diameter of 0.5 cm, with the total surface area of 7.5 cm² immersed in the solution and placed in the center of the cell. Cylindrical Ni foil placed close to the cell walls was used as a counter electrode providing excellent current distribution in the cell. Electrodeposition of powders was performed with a constant current regime using appropriate power supply. The deposition time was usually between 4 h and 5 h providing that the total concentration of the metal ions in the solution didn't change more than 10% and that the amount of electrodeposited powder was enough for SEM, X-ray and cross-section analysis. During the deposition process powder was removed from the electrode surface using gentle brush every 15–20 min. All solutions were made from distilled water and analytical grade chemicals. After deposition, powders were washed with distilled water and alcohol and left to dry in the air at room temperature.

X-ray powder diffraction (XRD) analysis of nickel and cobalt powders was carried out by a Siemens D500

diffractometer with a Ni filter and CuK_α radiation operated at a tube voltage of 35 kV and a tube current of 20 mA. A step scan mode was utilized with 0.02°2θ per step. The time step was 2 s. The angular 2θ range investigated was 5–100 deg (0.6°2θ min⁻¹).

The morphology of the electrodeposited powders was examined using scanning electron microscope (Philips, model XL30). Microstructural characterization of powders was performed using a Zeiss Axiovert 25 optical microscope. To observe the internal powder structure a loose powder with mounting epoxy resin mix was used. Samples were polished several times with the intention to reveal all possible types of particles and they are summarized in the analysis.

Results and discussion

Electrodeposited Ni powder

Nickel powder was electrodeposited from a solution containing 1 M (NH₄)₂SO₄, 0.7 M NH₄OH and 0.1 M NiSO₄ at a constant current density of 0.5 A cm⁻².

X-ray diffraction pattern of nickel powder sample is shown in Fig. 1a. As can be seen the powder consists only of the face-centered cubic nickel phase (β-Ni) with the lattice parameter of $a = 3.5231 \text{ \AA}$ (SD 0.0005). Crystallite size and lattice distortion are determined from the full width at half maximum (FWHM) [16, 17] of the X-ray peaks present on the diffractogram and corresponding results are presented in Table 1. As can be seen average size of crystallites of the β-Ni phase amounts to 40.89 nm. The standard values of the lattice parameters given in the parenthesis of Table 1 are taken from the Ref. [18].

Fig. 1 X-ray diffraction pattern of nickel (a) and cobalt (b) powder

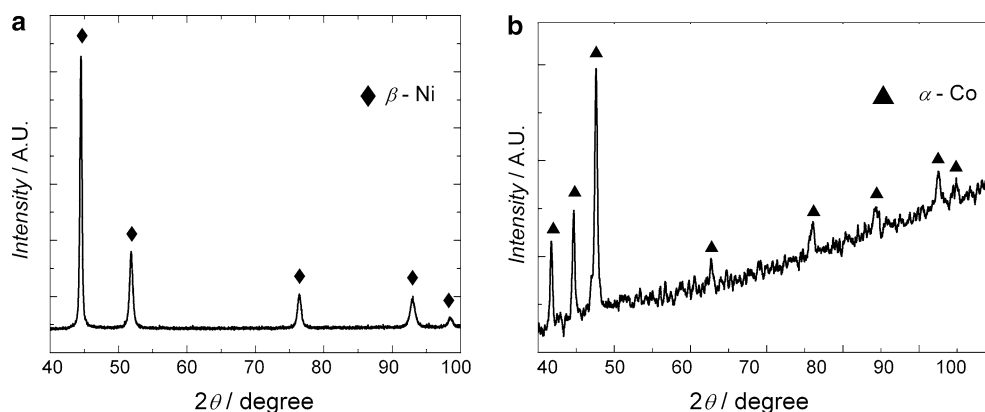


Table 1 Crystal structure, crystallite size, lattice distortion and lattice parameters of electrodeposited Ni and Co powders

Sample	Crystal Structure	Space group	Crystallite size (nm)	Lattice distortion (%)	Lattice parameters (nm)	
					<i>a</i>	<i>c</i>
Ni	FCC	<i>Fm3m</i>	40.89	0.065	0.35231 (0.35238)	
Co	HCP	<i>P63/mmc</i>	39.41	0.056	0.25007 (0.2507)	0.40563 (0.4070)

SEM micrograph of typical Ni powder particle is shown in Fig. 2. As can be seen typical cauliflower powder particles are obtained with the size of particles varying from about 5 μm to about 200 μm , no hydroxide impurities were detected, which is in accordance with the literature data [2, 5, 11]. Ni powder particles are very similar to those of copper [19a, 20] and since the mechanism of their growth has already been explained, it is not necessary to discuss the mechanism of Ni powder particles growth.

Electrodeposited Co powder

Cobalt powder was electrodeposited from a solution containing 1 M $(\text{NH}_4)_2\text{SO}_4$, 0.7 M NH_4OH and 0.1 M CoSO_4 at a constant current density of 0.5 A cm^{-2} .

X-ray diffraction pattern of cobalt powder sample is shown in Fig. 1b. As can be seen the powder consists only of the hexagonal close-packed α -cobalt phase with the lattice parameters of $a = 2.5007 \text{ \AA}$ (SD 0.0017) and $c = 4.0563 \text{ \AA}$ (SD 0.004). As in the case of Ni powder, no hydroxide or oxide impurities were detected. Crystallite size, lattice distortion and standard values of the lattice parameters, determined in the same way as in the case of Ni powder, are also given in Table 1. As can be seen average size of crystallites of the α -Co phase amounts to 39.41 nm.

In the case of Co powder electrodeposition, generally two types of particles are detected:

1. Dendrite particles varying in the size from about 5 μm to about 50 μm , as shown in Fig. 3a.
2. Different types of agglomerates varying in the size from about 100 μm to about 500 μm , as it is shown in Fig. 3 b, c, d. These agglomerates can further be divided into three groups:
 - (a) Compact agglomerates of the size of about 200 μm to about 500 μm , composed of smaller agglomerates of the size of about 20 μm to about

50 μm , Fig. 3b. These agglomerates are characterized with the presence of deep cavities and fern-like dendrites formed on the bottom of most of the cavities;

- (b) Spongy-like agglomerates of different shapes varying in the size from about 100 μm to about 200 μm with cavities, Fig. 3c.
- (c) Balls of the size of about 200 μm containing deep cavities with the fern-like dendrites formed on the bottom of most of the cavities and more or less dense cauliflower structure on the surface of these balls, as shown in Fig. 3d.

In the Figs. 4a–d and 5 a, b are shown cross sections of some of the particles detected in the Co powder deposit. As can be seen they are in good agreement with the SEM results: Fig. 4b ball-like particles; Fig. 4c spongy particles; Fig. 4d compact agglomerates.

Comparing morphology of Ni and Co powders, electrodeposited under the same conditions, it is obvious that powder particles are quite different. Although for Ni powder only one type, cauliflower-like particles is detected, while for Co powder different types of particles are present, it is quite obvious that only Co powder particles are characterized with the presence of large number of cavities. A common characteristic of these cavities for all types of agglomerates (Fig. 3) is the presence of small fern-like dendrites on the bottom of most of the cavities.

Considering cross-sections of some of the agglomerates detected in the Co powder deposit, Figs. 4 and 5 it is obvious that they are all different, not only because different types of agglomerates have been detected, but also because some pictures represent cross-sections of the agglomerate parallel to the line of its growth, while some pictures represent cross-sections of the agglomerate normal to the line of its growth. It has already been explained in the literature [21] that in the case of dendrite particles, depending on their length, it is possible that the morphology of the dendrite changes from

Fig. 2 SEM micrograph of electrodeposited Ni powder

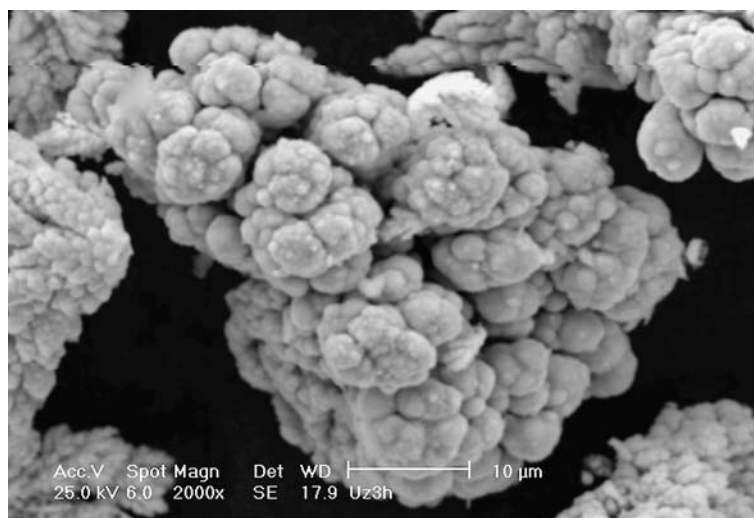


Fig. 3 SEM micrographs of **a** dendrite particles, **b** compact agglomerates, **c** spongy-like agglomerates and **d** ball-like agglomerates detected in the electrodeposited Co powder

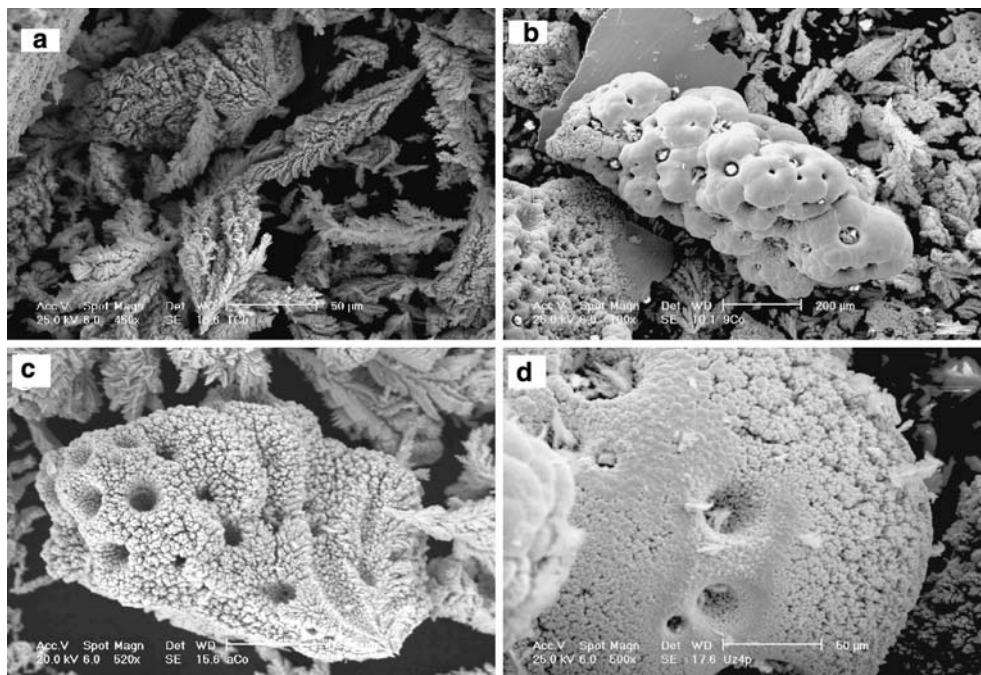


Fig. 4 Cross-section photographs of different particles detected in electrodeposited Co powder

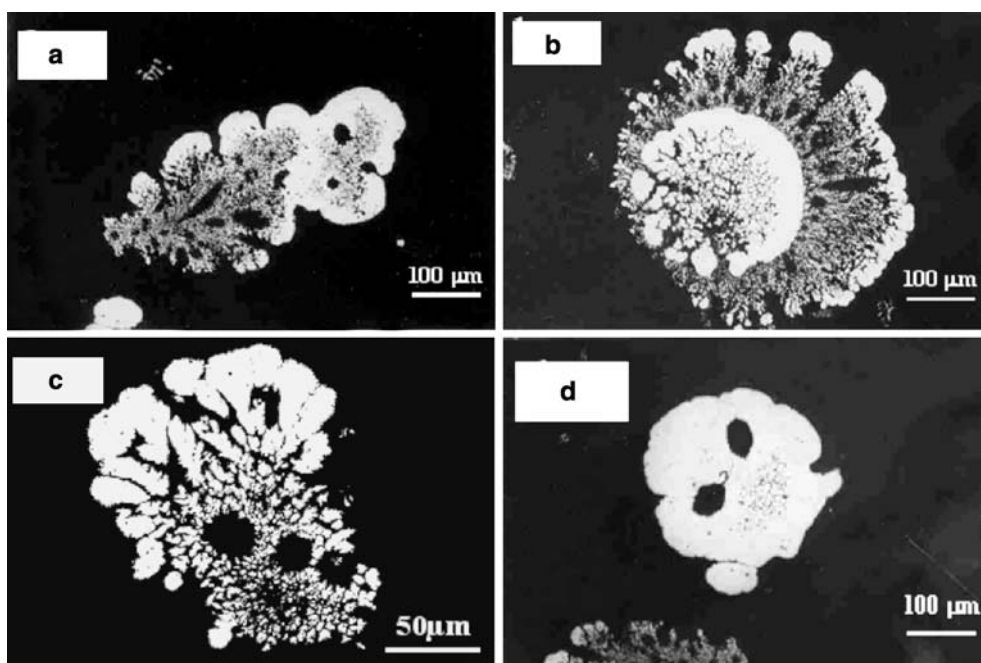
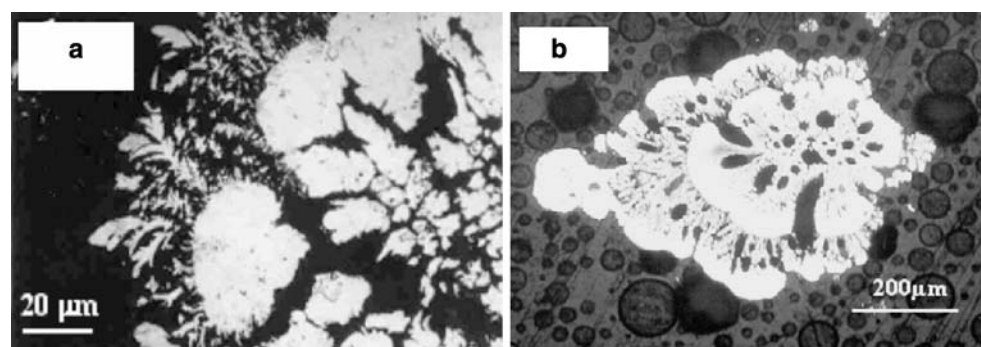


Fig. 5 Cross-section photographs of different particles detected in electrodeposited Co powder: **a** agglomerate with initial stage of the growth of second generation of dendrites, **b** agglomerate with two fronts of compact deposit



disperse one to a compact one in galvanostatic electro-deposition conditions, as it is shown in Fig. 4a. It is most likely that this cross-section represent the one parallel to the line of its growth. This agglomerate seems to grow from the left to the right side. With the time of growth the disperse agglomerate is branching in different directions and at the tip of each branch spherical diffusion is taking over the planar one, providing conditions for the growth of compact deposit as a consequence of the decrease of the local current density on the tip of each branch. After some time, these branches form compact deposit all over the agglomerate surface and the same agglomerate further grows as a compact one (right side of the particle), until it falls off from the electrode surface. In Fig. 4b it is most likely that a compact part of the agglomerate represents the picture of the cross-section normal to the line of its growth. Depending on the way of growth, the moment of falling off from the electrode surface and the position at the electrode surface where some agglomerate started to grow, different shapes of agglomerates are obtained (Fig. 4a–d), but all of them show the same characteristic of transforming disperse into compact deposit with increasing their size.

A special case is the formation of the balls of the size from about 200 μm containing deep cavities with the fern-like dendrites formed on the bottom of cavities and more or less dense cauliflower structure on the surface of these balls, Fig. 3d. The cross-section of such agglomerate is shown in Fig. 4b. For some reasons this agglomerate started to grow as a ball, again starting from disperse (in the middle) and finishing with compact deposit at the surface for a reason already explained. After some time of the growth of compact deposit the conditions for planar diffusion were restored causing the formation of disperse, dendrite particles all over the ball surface. It should be noted that at the same time there was a local increase of overpotential due to reduction of the active surface area as a result of compact deposit formation. Dendrites were growing normal to the ball surface and again, after some time spherical

diffusion took over the planar one and dendrites started transforming into compact deposit. Since dendrites were not dense, they were not able to form compact deposit all over the agglomerate surface when the agglomerates fall off from the electrode surface.

A cross-section of one of the agglomerates parallel to the line of its growth is shown in Fig. 5b. As can be seen, in accordance with the previous statement, after the first front of compact deposit has been formed, disperse deposit started to grow and for the same reasons its growth finished as a compact deposit at the moment when this agglomerate fall off from the electrode surface.

It is necessary to note that almost all morphological forms presented in this paper can be explained by the above discussion, being dependent on the stage of the agglomerates, i.e. the moment when they fall off from the electrode surface. It is most likely that the form presented in Fig. 6 should be considered as the initial stage of the growth of a second generation of dendrites, clearly detected on a cross-section of ball-like particles presented in Fig. 5a.

Quite unique feature of all agglomerates detected in Co powder deposit is the presence of deep cavities on their surface and the fern-like dendrites on their bottom for most of these cavities. This is illustrated in Figs. 3b and 6 for compact agglomerates and Fig. 3d for ball-like agglomerates. The most interesting one is the cavity detected in the ball-like agglomerates. More detailed micrograph for this cavity is shown in Fig. 7. It is most likely that these cavities are the consequence of hydrogen evolution and most probably a hydrogen bubble formation, preventing deposition inside the cavity. Once the bubble is liberated, the conditions for the growth of fern-like dendrites are fulfilled at the bottom of the cavity due to current distribution and restored planar diffusion. Since this agglomerate is not dense, crystals of different size can be seen in the cavity, with less dense ones placed at the bottom and more dense ones placed close to the top of the cavity. We believe that such distribution of crystals is the consequence of current

Fig. 6 SEM micrograph of the surface of the compact agglomerate with the initial stage of the growth of a second generation of dendrites

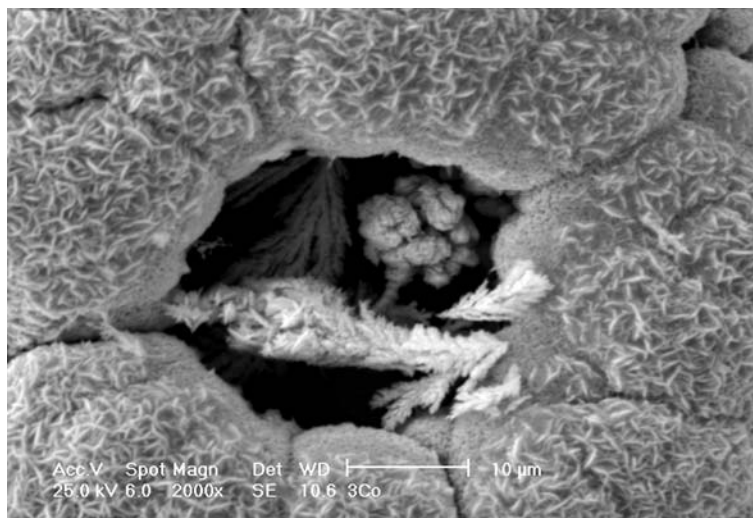
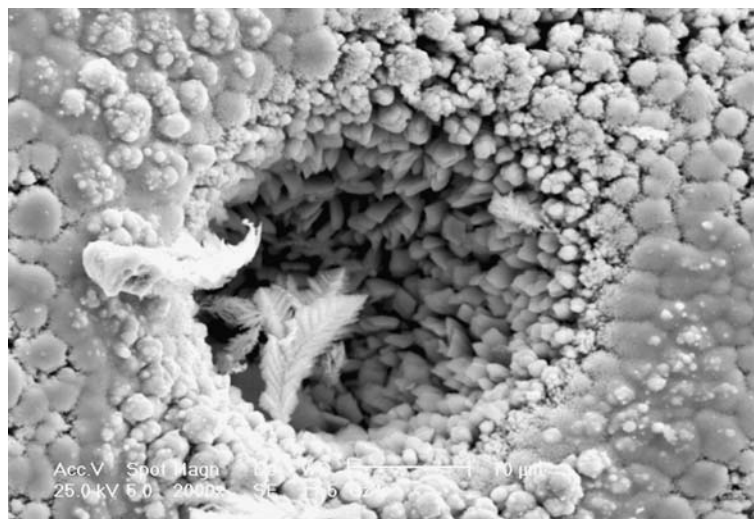


Fig. 7 More detailed SEM micrograph of the cavity detected on the ball-like agglomerate



distribution over the hydrogen bubble, while at the moment of bubble liberation fern-like dendrite starts growing at the bottom of cavity in the same way as the dendrites precursors in the diffusion layer of the macroelectrode [19b]. At that moment spherical diffusion is restored at the edges of cavity and compact deposit is obtained all around the cavity.

Concerning spongy deposits, it should be emphasized here that in comparison with other morphologies, traditionally called spongy, presented in the literature [22, 23] so far, the morphology of particles shown in Fig. 3c represents the real spongy deposit and that such similarity with the sponge has never been presented so far.

Finally, it should be emphasized here that the first results on the morphology, as well as on the internal structure (cross-section analysis), for electrodeposited Co powder are presented in this work.

Conclusions

From the results presented in this work it could be concluded that the morphology of electrodeposited Ni and Co powders is quite different. Ni powder is characterized by cauliflower-like type particles. In the case of Co powder, generally two types of particles are detected: (1) Dendrite particles and (2) Different types of agglomerates being characterized by the presence of cavities and fern-like dendrites formed on the bottom of most of them. These agglomerates can further be divided into three groups: (a) Compact agglomerates; (b) Spongy-like agglomerates of different shapes and (c) Balls of the size of about 200 μm with more or less dense cauliflower structure on their surface.

The growth mechanism of all agglomerates detected in the electrodeposited Co powder can be explained by a following reasoning: with the time of growth the disperse (dendrite) agglomerate is branching in different directions and at the tip of each branch spherical diffusion

takes over the planar one, providing conditions for the growth of compact deposit as a consequence of the decrease of the local current density on the tip of each branch. After some time, these branches form compact deposit all over the agglomerate surface and the same agglomerate further grows as a compact one, until it falls off from the electrode surface. The type of the agglomerate depends on its growth stage, i.e. on the moment when it falls off from the electrode surface.

It should be emphasized that the first results on the morphology of electrodeposited Co powder are presented in this work.

Acknowledgements This work was supported by the Ministry of Science and Environmental Protection of the Republic of Serbia under the research project "Electrodeposition of Metal Powders at a Constant and Periodically Changing Rate" (1806/2002).

References

- Calusaru A (1979) Electrodeposition of powders from solutions. Elsevier, New York
- Fedorova O (1938) Zh Obsch Khim 8:1711
- Hardy C, Mantell C (1937) FP No 815500
- Loshkarev M, Gernostaleva O, Kriukova A (1946) Zh Prikl Khim 19:739
- Levin A (1947) Collection of works of ural industrial institute (in Russian), p 125; (1946) Zhur Prikl Khim 19:779
- Hiruma K (1949) J Electrochem Soc Jpn 17:160
- Drozov B (1955) Zh Prikl Khim 1:45
- Nicol A (1946) CR 222:1043
- Wranglen G (1950) Acta Polytech Electr Eng Ser 2:69
- Kuroda M, Yto G, Shimizu Y (1953) Rept Sci Research (Japan) 29:429; Kuroda M, Yto G (1953) Japanese Patent No. 5166
- Mantell C (1941) USA Patent No. 2233103
- Pavlović MG, Hadžismajlović Dž, Popov KI (1991) Chem Ind (in Serbian) 45:239
- Mathers, Turner (1932) British Patent No. 403281
- Mathers (1932) Met Ind (NY) 30:321,396,368
- Huppomann WJ, Dalal K (1986) Metallographic atlas of powder metallurgy. Werlag Schmid GmbH, pp 21–63
- Lönnerberg B (1994) J Mat Sci 29:3224
- Ziegler G (1978) Powder Met 10:70

18. X-ray powder JCPDS diffraction files 5-0727, 4-0850
19. Popov KI, Krstajić NV, Čekerevac MI (1996) In: White RE, Conway BE, Bockris JO'M (eds) Modern aspects of electrochemistry. vol 39, Chap 6. Plenum, New York (a) p 319, (b) p 298
20. Popov KI, Krstić SB, Obradović MČ, Pavlović MG, Pavlović LjJ, Ivanović ER (2004) J Serb Chem Soc 69:43
21. Murashova IB, Pomošov AV (1989) Electrodeposition of metals in the form of dendrites (in Russian). In: Itogi nauki i tehniki Seria Elektrokimiya vol 30. VINITI, Moskva, p 90
22. Popov KI, Krstajić NV (1983) J Appl Electrochem 13:775
23. Popov KI, Krstajić NV, Simičić KV, Babić NM (1992) J Serb Chem Soc 57:927